Carbon Science

Vol. 1, No. 3 & 4 January 2001 pp. 133-137

Preparation and Electric Double Layer Capacitance of Mesoporous Carbon

Soshi Shiraishi♠, Hideyuki Kurihara and Asao Oya

Department of Chemistry, Faculty of Engineering, Gunma University, Tenjin-cho 1-5-1, Kiryu, Gunma 376-8515, Japan

♠e-mail: *ssiraisi@chem.gunma-u.ac.jp*

(Received December 14, 2000; accepted December 20, 2000)

Abstract

Mesoporous activated carbon fiber (ACF) was prepared from phenolic resin containing a small amount (0.1 wt %) of organic nickel complex through carbonization and steam activation. Microporous ACF as reference sample was also prepared from phenolic resin without agent. In both cases of the mesoporous ACFs and the microporous ACFs, the electric double layer capacitance of the nonaqueous electrolyte (0.5 M $TEABF_4$/PC or 1.0 M $LiClO_4$/PC) was not proportional to the BET specific surface area. This is owing to the low permeability of nonaqueous electrolyte or the low mobility of ion in narrow micropores. However, the mesoporous ACF showed higher double layer capacitance than the microporous (normal) ACF. This result suggests that the presence of many mesopores promotes the formation of effective double layer or the transfer of ion in the micropore.

Keywords : *Mesopore, Activated Carbon Fiber, Electric Double Layer Capacitance, Nonaqueous Electrolyte*

1. Introduction

The electric energy storage system utilizing charge-discharge process of electric double layer on porous electrode is called "Electric double layer capacitor (EDLC)" [1, 2], which has been used as memory back-up device because of its high cycle efficiency and the long cycle life. Moreover, recently, EDLC is expected as the sub power source for hybrid electric vehicle (HEV) for EDLC's higher power density (larger than 1000 W kg^{-1}). However, since the energy density of EDLC is quite lower (several $Whkg^{-1}$) than that of rechargeable batteries, the capacitance of EDLC has to be increased. The practical electrode material for EDLC is porous carbon such as activated carbons. The high capacitance (100~200 Fg^{-1}) is owing to high specific surface area (>1000 m^2g^{-1}) produced by many micropores (2 nm > pore width [3]). In general, it is believed that there is a proportional relationship between the specific surface area and the electric double layer capacitance of activated carbons [1, 4, 5]. However, in fact, some researchers have reported nonlinearity of the double layer capacitance on the surface area [6-14]. This may be concerned with the pore size distribution (PSD) and the kinds of ion or solvent in electrolyte. The PSD depends on the carbon precursor and the preparation method of porous carbon. Especially, mesopores (2 nm < pore width < 50 nm [3]) or macropores (pore width > 50 nm [3]) should not be ignored because they can influence the permeation of electrolyte to microporous structure or the mobility of ion in pore. In the meantime, recently, special activated carbon fiber (ACF) containing mesopores was prepared by blending activation catalyst with carbon precursor (phenolic resin [15] or isotropic pitch [16]). Since ACF prepared normally is known to be excellent microporous carbon without larger pores such as mesopore or macropore [17, 18], mesoporous ACF is a suitable material to investigate the influence of mesopore on the double layer capacitance. Therefore, in this paper, the double layer capacitance of mesoporous ACF is discussed in terms of a comparison with normal ACF.

2. Experimental

2.1. Preparation and Characterization of ACF

Generally, mesoporous ACF can be obtained through activation process of carbon fiber containing activation catalyst [15, 16]. In this study, the mesoporous ACF was prepared by "blending method" [15, 19] as described in the following. Nickel was selected as activation catalyst. Novolac-type phenolic resin (obtained from Gun-Ei Chemical Industry Co., Ltd., Japan) and bis(2.4-pentanedionate) nickel(II) dihydrate (nickel acetylacetonate dihydrate, $(CH_3COCHCOCH_3)_2$-$Ni{\cdot}2H_2O$, Wako Chemical, Japan) were dissolved in methanol, where the percentage of nickel in raw materials was 0.1 wt %. The methanol was removed under a reduced pressure to obtain a mixture resin. The resin was spun centrifugally to prepare resin fiber. After stabilization of the resin fiber, it was heated to 800°C in nitrogen atmosphere and continuously activated in steam at 800°C. The ACF without agent (pristine fiber) was also prepared in the same way as the above preparation process. The samples containing Ni species and without agent were referred to as "0.1Ni-ACF (acti-

vation time)" and "Ref-ACF (activation time)", respectively. X-ray diffraction (XRD) measurement revealed that nickel species in 0.1 Ni-ACFs were loaded as metallic nickel particles (crystallite size 40 nm). The pore characterization of these ACFs was performed by N_2 adsorption/desorption system (BELSORP28SA, BEL JAPAN, Inc., Japan).

2.2. Measurement of electric double layer capacitance of ACF

The composite pellet electrode was prepared from ground ACF (about 0.05 g), acetylene black (Denki Kagaku Kogyo, Co., Japan), and binder (PTFE 6J, Du Pont–Mitsui Fluorochemicals Co., Ltd., Japan). The ratio of ACF, acetylene black, and binder in the electrode was 90 : 10 : 5 wt%, respectively. The composite electrode was put on titanium mesh as current collector. The standard three-electrode cell was used to measure the electric double layer capacitance of single ACFs electrode. The electrode was degassed in electrolyte under a vacuum ($<10^3$ Pa) to penetrate electrolyte to pores before electrochemical measurement. The charge-discharge cycle was conducted at galvanostatic condition (40 mA g^{-1}) in nonaqueous electrolyte. Propylene carbonate containing 0.5 mol dm^{-3} tetraethylammonium tetrafluoroborate ($(C_2H_5)_4NBF_4$) electrolyte (0.5 M $TEABF_4$/PC) or propylene carbonate containing 1.0 mol dm^{-3} $LiClO_4$ electrolyte (1.0 M $LiClO_4$/PC) was used as nonaqueous electrolyte. In this paper, anodic (cathodic) process is referred to as charge (discharge) process. The electric double layer capacitance was calculated by the amount of electricity passed during charge or discharge process as the following equation.

$$C = i\,t / w\Delta V \quad (1)$$

where C; electric double layer capacitance [F g^{-1}], i; current [A], t; charge (or discharge) time [s], w; weight of ACF in the electrode [g], and ΔV; potential change during charge (or discharge) process [V] (= 2 V, in this study).

The capacitance obtained by equation (1) corresponds to the specific gravimetric electric double layer capacitance of the ACFs.

3. Results and Discussion

3.1. Pore Structure

The N_2 adsorption/desorption isotherms of both of Ref-ACF (480) and 0.1 Ni-ACF (180) were shown in Fig. 1. In the isotherm of the Ref-ACF (480), a large amount of N_2 was adsorbed remarkably at low relative pressure (< 0.1 P/Ps), while the N_2 adsorption was saturated at middle and high P/Ps. Therefore, the isotherm of the Ref-ACF (480) can be considered as a typical one (Type I) for microporous carbon. The drastic increment of adsorption in the low relative pressure is due to the micropore filling effect [3, 20]. On the other hand, in the case of 0.1Ni-ACF (180), the amount of N_2 adsorption gradually still increased in the region of middle P/Ps and markedly increased in the region of high P/Ps such as > 0.8 P/Ps. This result can be attributed to the capillary condensation of N_2 in mesopore (or macropore). The pore size distributions (PSD) of mesopores for Ref-ACF (480) and 0.1 Ni-ACF (180) were shown in Fig. 2. These PSDs were calculated by the adsorption isotherms using Dolimore-Heal (DH) method [21]. The PSD exhibited that more mesopores were included in 0.1 Ni-ACF (180) than those in Ref-ACF (480). Especially, 0.1 Ni-ACF (180) had much pore volume of relatively large size mesopore such as 10~40 nm pore. The Brunauer-Emmett-Teller specific surface area (BET-SSA, corresponding to total specific surface area of ACFs) and the DH pore volume (DH-PV, corresponding to total pore volume of mesopores in the ACFs) were summarized in Table 1. In both of Ref-ACFs and 0.1Ni-ACFs, the BET specific surface area was increased as

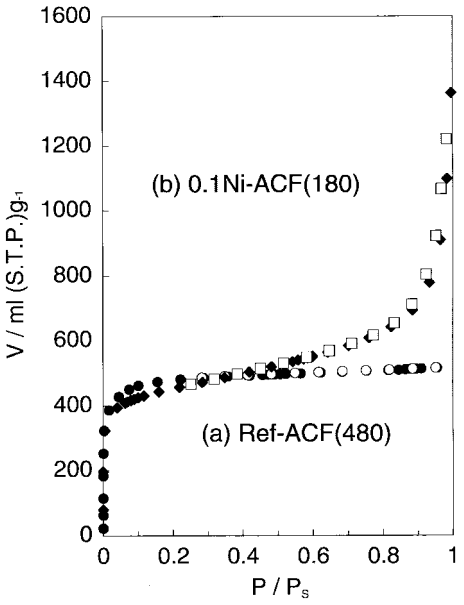

Fig. 1. N_2 adsorption and desorption isotherms (77K) of (a) Ref-ACF (480) and (b) 0.1Ni-ACF (180), the BET surface areas of Ref-ACF (480) and 0.1Ni-ACF (180) are 1776 m^2 g^{-1} and 1655 m^2 g^{-1}, respectively. Filled symbols: adsorption isotherms, open symbol: desorption isotherms.

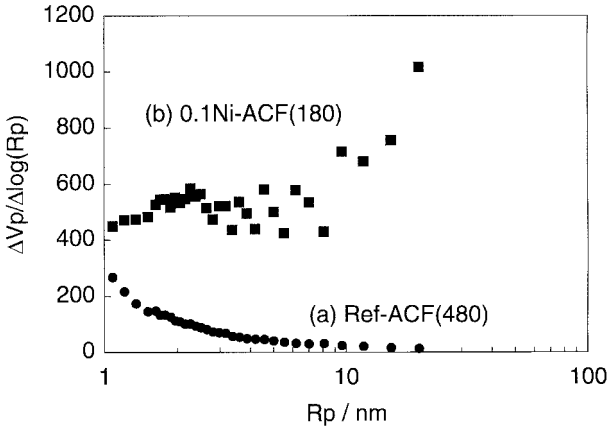

Fig. 2. Pore size distribution for the mesopore region of Ref-ACF (480) and 0.1Ni-ACF (180), calculated by the DH method. Rp; pore radius, Vp; pore volume.

Table 1. Summary of samoke sites and designation of samples

Age	Formation	Site name	No. of samples (clast)	Lithology	*Schistosity		**Lineation on the schistosity plane
Unknown (Late Pre Cambrian to Early Paleozoic?)	Hwanggangri Formation	H1	15(6)	Dark grey pebble-bearing phyllite (Originally pebble-bearing silt and mudstone) Poorly sorted and matrix-supported	S_1	56/40	66/11
					S_2	39/52	?
		H2	13(4)		S_1	183/28	263/28
					S_2	115/10	?
		H3	9(0)		S_1	287/13	297/02
					S_2	13/38	58/31
		H4	13(0)		S_1	217/41	22/13
					S_2	04/34	?
		H5	12(2)		S_1	198/37	276/32
					S_2	08/32	?
		H6	19(9)		S_1	44/55	66/28
					S_2	29/75	?
		H7	10(0)		S_1	80/54	?
					S_2	55/56	?
		H8	11(0)		S_1	57/63	?
					S_2	38/88	217/22
		H9	9(0)		S_1	58/37	?
					S_2	41/74	?
		H10	11(0)		S_1	227/50	?
					S_2	41/63	?
		H11	11(0)		S_1	?	?
					S_2	54/66	?
		H12	12(0)		S_1	337/60	?
					S_2	94/17	?
		H13	19(0)		S_1	106.47	?
					S_2	56/56	?
		H14	14(0)		S_1	268/63	?
					S_2	246/80	?
		H15	10(0)		S_1	218/36	?
					S_2	38/56	?

*Strike/dip and **azimuth/plunge are measured according to the right-hand rule. ?: not possible to measure/not sufficiently developed.

the activation duration was extended. This means that the pore structure in the ACFs is developed well with longer activation time. The mesopore volume in Ref-ACFs was increased slightly through the activation, while the mesopore volume in 0.1Ni-ACFs was markedly changed by the activation from approximately 100 to 860 $mm^3\ g^{-1}$. Especially, 0.1 Ni-ACF had larger mesopore volume compared with Ref-ACF having the almost same BET specific surface area. Additionally, the total micropore volume (W) and average micropore width (2χ) were estimated by the adsorption isotherms using Dubinin–Radushevich (DR) equation [22, 23]. They were also summarized in Table 1. The micropore volume and the micropore width became larger with longer activation duration in the case of both of Ref-ACF series and 0.1Ni ACF series. However, little difference was observed in the micropore volume and the average micropore width between Ref-ACF and 0.1Ni-ACF with the almost identical BET surface area (for example, Ref-ACF (480) and 0.1Ni-ACF (180)). These results suggested that the growth of micropore structure was independent of the mesopore formation under the activation catalyst. Therefore, it can be concluded that 0.1Ni-ACFs are special ACFs containing not only many mesopores but also many micropores and that large specific surface area of 0.1Ni-ACF is due to the devel-

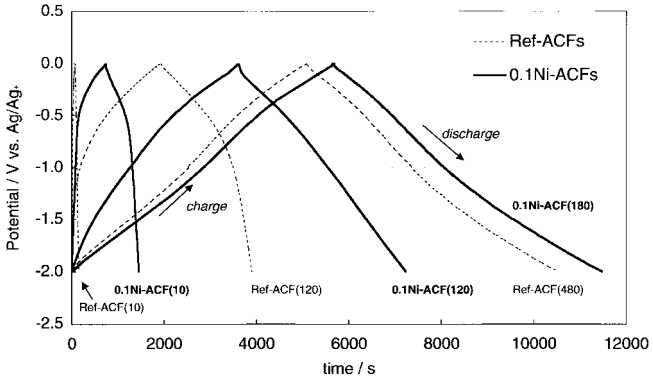

Fig. 3. Potential-time curve for Ref-ACFs and 0.1Ni-ACFs in 0.5 mol dm^{-3} $(C_2H_5)_4NBF_4$/propylene carbonate. Galvanostatic method (40 mAg^{-1}), potential range; –2 V~0 V vs. Ag/Ag^+.

oped micropore structure.

3.2. Electric Double Layer Capacitance of ACF

Fig. 3 shows that potential-time curve for Ref-ACFs and 0.1Ni-ACFs in 0.5 M $TEABF_4$/PC electrolyte. The electrode potential of Ref-ACF (480), 0.1Ni-ACF (120), and 0.1Ni-ACF (180) was changed linearly by the amount of electricity passed for the charge or discharge process. Any plateaus derived from electrochemical reaction such nickel dissolution were not observed in the curves of 0.1Ni-ACF (120) and 0.1Ni-ACF (180). Therefore, these ACF electrodes can be considered as a polarizable electrode with a constant capacitance. On the other hand, the potential-time curves of Ref-ACF (120) and 0.1Ni-ACF (10) were distorted. Considering the slope of the curve corresponds to the capacitance, it means that the double layer capacitance of these ACF electrodes depended on the potential during charge or discharge. The potential-dependence may be derived from the difference in the capacitance between anion adsorption/desorption process (upper region of initial potential) and cation adsorption/desorption process (lower region of initial potential) since initial potential of all electrodes showed around –1.0 V vs. Ag/Ag^+. The capacitance was estimated by equation (1) to discuss the relationship between the BET-SSA and the double layer capacitance in detail.

Fig. 4 is the relationship between the BET specific surface area (BET-SSA) and the electric double layer capacitance (potential range was -2 V~0 V vs. Ag/Ag^+) in 0.5 M $TEABF_4$/PC. In both cases of Ref-ACFs and 0.1Ni-ACFs, the double layer capacitance was not linearly proportional to the BET SSA. The quite small capacitance of the ACFs with small BET-SSA (ex., Ref-ACF (10) or 0.1Ni-ACF (10)) is derived from difficulty in forming effective double layer or low mobility of ion in narrow micropores. However, the double layer capacitance of 0.1Ni-ACF was higher than that of Ref-ACF with the almost same BET–SSA (ex., Ref-ACF (60) vs. 0.1Ni-ACF (60), or Ref-ACF (120) vs. 0.1Ni-ACF (120)). Especially, the higher capacitance of 0.1Ni-ACFs was prominent in the region between 1000~1500 m^2g^{-1} BET-SSA. In the previous section, the followings have been

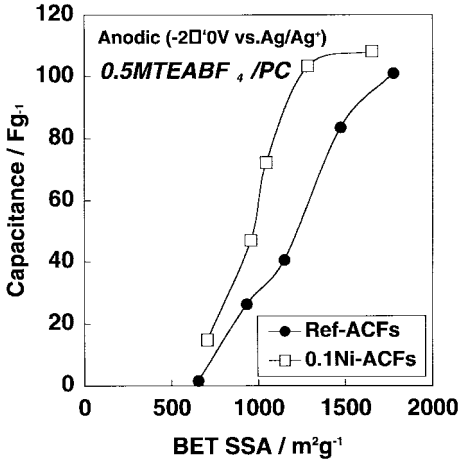

Fig. 4. Relationship between BET specific surface area and electric double layer capacitance (charge process) for Ref-ACFs and 0.1Ni-ACFs in 0.5 mol dm^{-3} $(C_2H_5)_4NBF_4$/propylene carbonate. Galvanostatic method (40 mAg^{-1}), potential range; –2 V~0 V vs. Ag/Ag^+.

revealed. 1) The mesopores in Ni-ACF series were developed much well compared with Ref-ACFs. 2) There was little difference in micropore structure for both of the Ref-ACFs and 0.1Ni-ACFs in terms of the average micropore width and the micropore volume. Therefore, this advantage of the capacitance of 0.1N-ACFs can be attributed to the presence of many mesopores, which assists to the permeation of nonaqueous electrolyte in pore or the transfer of ion through microporous structure.

Fig. 5 showed the relationship between the BET specific surface area (BET-SSA) and the electric double layer capacitance (potential range was 2 V~4 V vs. Li/Li^+) in 1.0M $LiClO_4$/PC. The initial potential of the ACF electrode was around 3 V vs. Li/Li^+, so the essential potential range during charge/discharge process was roughly not different between

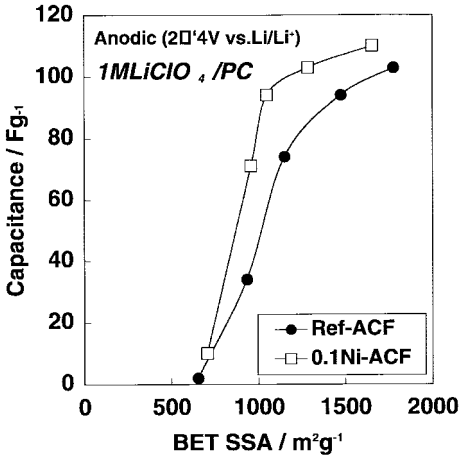

Fig. 5. Relationship between BET specific surface area and electric double layer capacitance (charge process) for Ref-ACFs and 0.1Ni-ACFs in 1.0 mol dm^{-3} $LiClO_4$/propylene carbonate. Galvanostatic method (40 mAg^{-1}), potential range; 2 V~4 V vs. Li/Li^+.

$TBABF_4$/PC electrolyte and $LiClO_4$/PC. The non-linearity of capacitance on the BET-SSA and the higher capacitance of 0.1Ni-ACFs were observed in $LiClO_4$/PC electrolyte as well as in $TEABF_4$/PC electrolyte. However, the capacitance of 0.1Ni-ACF and, especially, Ref-ACF in $LiClO_4$/PC electrolyte was somewhat higher that in $TEABF_4$/PC electrolyte. Stokes radius (=solvated-ion radius) of TEA^+, Li^+, BF_4^-, or ClO_4^- can be estimated to be 0.36 nm, 0.41 nm, 0.24 nm, or 0.26 nm, respectively, by the single ion limiting molar conductivity [24] in PC. Thus, there is little difference in stokes radius between the cations (TEA^+ and Li^+) or the anions (BF_4^- and ClO_4^-), so the superiority of $LiClO_4$/PC electrolyte on the double layer capacitance does not seem to be caused by the ion size effect on pore width. However, it is not reasonable to suppose the transfer of solvated ion in micropore as bulk electrolyte. Considering the ionic radius of Li^+ is very small (0.08 nm) [24], the solvated Li^+ ion can vary the dimension by desolvation or rearrangement of solvent cage. On the other hand, the ionic radius (0.34 nm) of TEA^+ is not different from its Stokes radius [24]. Therefore, the higher capacitance of $LiClO_4$/PC electrolyte may be due to the smooth transfer of Li^+ ion in micropores. The "flexibility" of solvated Li^+ ion compared with TEA^+ ion was also discussed in the recent report of Soffer and Aurbach's group [14]. We are also now investigating the influence of the pore structure in ACF and the kind of ion on the double layer capacitance in detail.

References

[1] Conway, B. E. "*Electrochemical Super Capacitors*", Kluwer Academic/Plenum Publishers, New York, **1999**.

[2] Nishino, A. *J. Power Sources* **1996**, *60*, 137.

[3] Gregg, S. J.; Sing, K. S. W. "*Adsorption, Surface Area and Porosity*", Academic Press, London, **1982**.

[4] Takahashi, I.; Yoshida, A.; Nishino, A. *Denki Kagaku (presently Electrochemistry)* **1988**, *56*, 892.

[5] Morimoto, T.; Hiratsuka, K.; Sanada, Y.; Kurihara, K. *J. Power Sources* **1996**, *60*, 239.

[6] Shi, H. *Electrochim. Acta* **1996**, *41*, 1633.

[7] Qu, D.; Shi, H. *J. Power Sources* **1998**, *74*, 99.

[8] Iwasaki, S.; Okusako, Y.; Miyahara, M.; Okazaki, M. *Kagaku Kogaku Ronbunshu* **1997**, *23*, 512 (in Japanese).

[9] Lin, C.; Ritter, J. A.; Popov, B. N. *J. Electrochem. Soc.* **1999**, *146*, 3639.

[10] Nakagawa, H.; Shudo, A.; Miura, K. *J. Electrochem. Soc.* **1999**, *147*, 38-42.

[11] Sakata, Y.; Muto, A.; Uddin, M.A.; Yamada, N.; Marumo, C.; Ibaraki, S.; Kojima, K. *Electrochem. Solid-State Lett.* **2000**, *3*, 1.

[12] Yoon, S.; Lee, J.; Hyeon, T.; Oh, S. M. *J. Electrochem. Soc.* **2000**, *147*, 2507.

[13] Shiraishi, S.; Kurihara, H.; Tsubota, H.; Oya, A.; Soneda, S.; Yamada, Y. *Electrochem. Solid-State Lett.* **2001**, *4*, A5.

[14] Salitra, G.; Soffer, A.; Eliad, L.; Cohen, Y.; Aurbach, D. *J. Electrochem. Soc.* **2000**, *147*, 2486.

[15] Oya, A.; Yoshida, S.; Alcaniz-Monge, J.; Linares-Solano, A. *Carbon* **1995**, *33*, 1085.

[16] Tamai, H.; Kakii, K.; Hirota, Y.; Kumamoto, T.; Yasuda, H.; *Chem. Mater.* **1996**, *8*, 454.

[17] Suzuki, M. *Carbon* **1994**, *32*, 577.

[18] Ryu, S. K. *High Temperature-High Pressures* **1990**, *22*, 345.

[19] Przepiorski, J.; Oya, A. *J. Mater. Sci. Lett.* **1998**, *17*, 679.

[20] Kaneko, K.; Ishii, C.; Ruike, M.; Kuwabara, H. *Carbon*, **1992**, *30*, 1075.

[21] Dollimore, D.; Heal, G. R. *J. Applied Chem.* **1964**, *14*, 109.

[22] Dubinin, M. M.; Stoeckli, H. F. *J. Colloid Interface Sci.* **1980**, *75*, 34.

[23] E.–Merraoui, M.; Tamai, H.; Yasuda, H.; Kanata, T.; Mondori, J.; Nadai, K.; Kaneko, K. *Carbon* **1998**, *36*, 1769.

[24] Ue, M. *J. Electrochem. Soc.* **1994**, *141*, 3336.